

Patterns in Pupillary Diameter Variation While Reading Portuguese Language Texts

João Vitor Macedo Romera^a, Rafael Nobre Orsi^b and Carlos Eduardo Thomaz^c

Departamento de Engenharia Elétrica, Centro Universitário FEI, Avenida Humberto de Alencar Castelo Branco, Brazil

Keywords: Pupil, Cognition, Meares-Irlen Syndrom, Signal Processing.

Abstract: This work investigates patterns of pupil diameter variation during text reading based on the effects of Meares-Irlen Syndrome (MIS) using eye tracking information to estimate the mental workload required. The results show that there is an increase in the mental workload at times when the texts presented had greater intensity of visual distortion and that it is possible to linearly classify the data by multivariate statistical techniques, disclosing experimentally the implicit difficulty in such reading context.

1 INTRODUCTION

An ability to read involves countless cognitive processes, from the acquisition of visual information by the eyes to the cognitive processing of information by the brain (Orsi et al., 2019). However, an ability to read is only executed efficiently if all cognitive processes function properly. If there are failures in any process, the subject may present difficulties when performing the reading task, as is the case of Meares-Irlen Syndrome (MIS) (Irlen, 1990), a sensory deficiency that affects the acquisition of visual information, resulting in low reading performance because of visual distortions, reflecting in problems in the learning process, especially during the childhood.

With the advance of science and technology, it has become possible to analyze and model the processes required for the execution of the reading task, enabling deeper analyses of how it works, revealing possible anomalies in the functioning of some of those processes for those individuals who present difficulties in reading. A novel and recent analysis that can be considered is the pupil diameter analysis, an involuntary sign which directly reflects the mental effort demanded during the execution of any task.

The present work focuses on analyzing the pupil diameter variation during the reading of texts that simulate the visual effects of MIS, investigating the relationship between pupil diameter and the quality of

the information presented in the text, in order to estimate the mental effort required in reading tasks for those with MIS.

2 FUNDAMENTAL CONCEPTS

This section presents the fundamental concepts for understanding the effects caused by MIS that inspired the experiment and the analysis of mental effort by measuring pupil diameter.

2.1 Meares-Irlen Syndrom (MIS)

MIS is described as a disorder that affects the perception of visual stimuli and causes scene distortion, affecting mainly the ability to read, which becomes slow and discontinuous (Irlen, 1990). The individuals who suffer most from these consequences are mainly children who are during the learning process, reflecting low school performance and difficulties in interpersonal relationships (Soares and Gontijo, 2016). Besides social issues, people with this syndrome also report eye irritation, hypersensitivity to light, headaches, and visual stress (Irlen, 1990).

It is estimated that 45% of people with reading difficulties have a positive diagnosis for the syndrome, so it is often confused with other deficits that influence reading ability, such as Dyslexia and ADHD. (Bicalho et al., 2015). Because of this, the identification of the syndrome becomes a difficult task, mainly because it is still identified through psychological

^a <https://orcid.org/0000-0002-9331-8880>

^b <https://orcid.org/0000-0003-4719-0131>

^c <https://orcid.org/0000-0001-5566-1963>

procedures, such as comprehension and efficiency in reading text, which considers very simplistic quantitative metrics like the count of words read per minute (Irlen, 1990).

There are still few studies that identify the discriminating characteristics present in the ocular signs of people with the syndrome (Romera et al., 2019) (Guimarães et al., 2020) (de Faria, 2011). However, recent approaches that explore eye-tracking tools are presenting new findings on the behavior of individuals with the syndrome, making it possible to identify patterns from data such as eye movements, regressions, saccades and pupil diameter changes (Romera et al., 2019).

2.2 Mental Effort and Pupillary Measurement

The human eye is composed of several parts that, by means of visible light, capture the visual information present in the environment. One of these parts is the pupil, which is an orifice through which light enters and which has a diameter that can be regulated by two iris muscles: the sphincter muscle, which is innervated by the parasympathetic part of the ANS (Autonomic Nervous System) and is responsible for pupil constriction, and the dilator muscle, which is innervated by the sympathetic part of the ANS and is responsible for pupil dilation (Marieb and Hoehn, 2007). The constriction and dilation are caused by two factors: (1) to control the luminosity that enters the eye, protecting the photoreceptor cells present in the retina, which are responsible for sending information by means of electrical impulses to the brain via the optic nerves and, (2) by an involuntary reflex of the ANS during the transition between states of attention and rest that regulate the amount of information captured by the eyes (Beatty et al., 2000)(Senior et al., 2010)(Bremner, 2012). For the second case, the pupil diameter signals can become a signal that indicates the individual's mental states, reflecting the mental effort required to perform some task. In the case of increased mental effort, the pupil reveals the state of attention, receiving the ANS sympathetic signal for pupil dilation, acquiring a larger amount of visual information while performing the task, whereas in the case of decreased cognitive effort, the pupil reveals the state of rest and energy saving, receiving a parasympathetic signal for pupil constriction, acquiring a smaller amount of visual information, as shown in Figure 1 (Orsi et al., 2019).

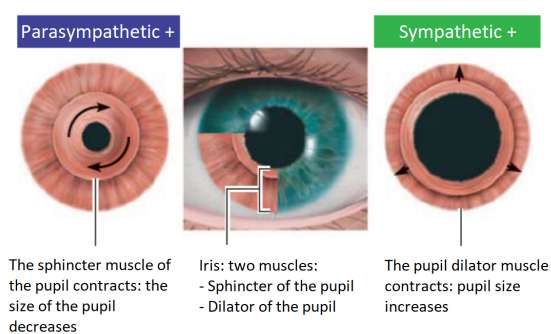


Figure 1: Iris muscles. Adapted from (Marieb and Keller, 2011).

3 METHODS

This section describes the set of materials and methods used to perform the experiment and to process the pupil signal, divided into 7 subsections: visual stimulus; reading experiment; signal acquisition, signal preprocessing, image preprocessing, frequency domain analysis and pattern recognition.

3.1 Visual Stimulus

From reports of individuals with the syndrome, the most common visual distortions during the reading of static texts are blurry and washout (Irlen, 2005). The initial phase of the experiment consisted in generating videos simulating these effects, to be later presented to volunteers on a computer screen equipped with an eye-tracking device. To perform this step, a code was developed in the R language, using the image processing library "Magick" that generated a dynamic animation in .avi format that distorted cyclically from the insertion of a text as input, intensifying and smoothing within periods of time. The texts selected were children's stories with a low level of complexity so that there would be no bias in less skilled individuals or those with little grammatical knowledge.

The results were two videos, each simulating a different visual distortion (blurry and washout) that a voluntary person can perceive when reading a static text, as presented in Figures 2 and 3.

The intensity of the effects was defined with a distortion parameter, ranging from 0 to 1, where 0 is the scale with no visual distortion and 1 is the maximum visual distortion.

3.2 Reading Experiment

The experiment included 70 participants, 30 men and 40 women, all healthy and cognitively able. In ad-

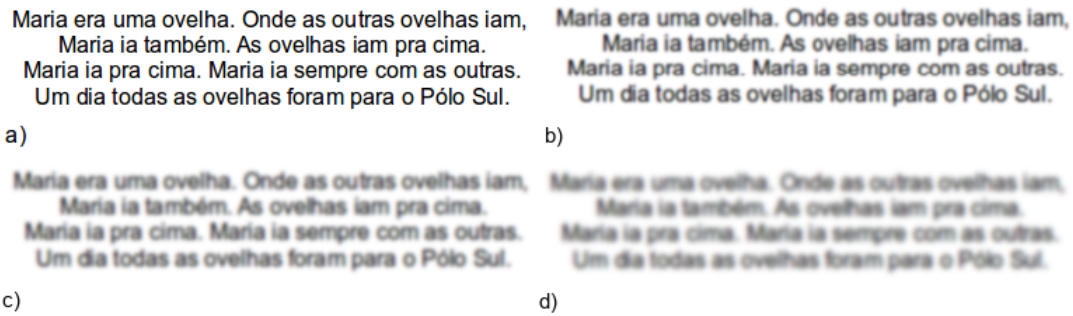


Figure 2: Coded Blurry effect.

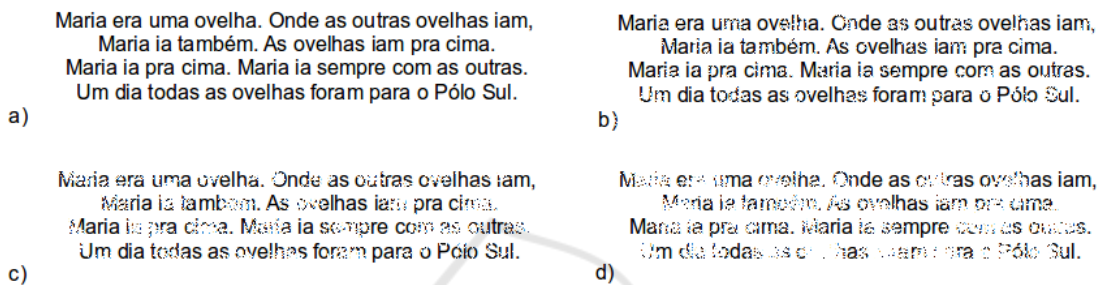


Figure 3: Coded Washout effect.

dition, the sample had a mean age of 17.89 years and a standard deviation of 7.95 years. The sample went through a filtering stage, selecting only adolescent participants, aged between twelve and eighteen years old (Federal, 1990), resulting in a sample with 50 signals with a mean age of 16.9 years and a standard deviation of 6.82 years.

The initial phase of the experiment consisted of settling the participant in, instructions for performing the steps of the experiment, and calibration of the eye-tracking equipment (Tobii TX 300), as presented in Figure 4.

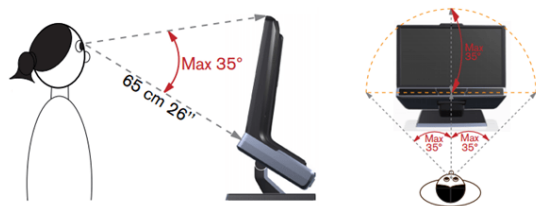


Figure 4: Calibration example of eye-tracking equipment (Orsi et al., 2019).

The experiment had 3 stages, and in each stage a text containing a visual effect was presented, followed by an inferential question to make sure that the volunteer really read the text. In the first stage the text without visual distortion was always presented so that the natural reading pattern of each volunteer could be identified. Then the other texts were pre-

sented with the simulated distortion effects. The texts had a predefined display time, 32 seconds for the text without any effect, 32 seconds for the text with blurry effect (oscillating every 8 seconds), and 36 seconds for the text with washout effect (oscillating every 9 seconds). The display periods were defined based on the average reading time of each text obtained empirically, through tests performed in the laboratory. The questions referring to the text had a free time for answering, and they were asked to be answered verbally. As soon as the volunteer verbalized the answer, an instructor wrote down the answer and asked the participant to press any key on the keyboard in front of him to begin the next step of the experiment.

3.3 Signal Acquisition

The signal acquisition was performed indoors with artificially controlled lighting within the optimum specifications between 300 and 1000 lux (Bergstrom and Schall, 2014). The equipment used was the Tobii TX300 eye-tracker along with a notebook computer with a Core i7 processor and 16 Gb of RAM and Windows 7 operating system.

3.4 Signal Preprocessing

After the acquisition step, all signals are exported individually from Tobii Studio, which is the official software of the eye tracking equipment used. Then a

code developed in Python programming language is used to extract the pupil diameter measurements of each participant during the reading of each text, generating 3 signals for each participant, resulting in a total of 150 pupil signals, being 50 signals for each effect (Neutral, Blurry and Washout). Considering that during the reading experiment the participants blinked, the signal is preprocessed by means of linear interpolation and, after the interpolation step, the signals are smoothed using the Savitzky-Golay filter of order 2 with window size 200 (Savitzky and Golay, 1964). Figure 5 shows the original signal from a participant captured by the eye tracker and the filtered signal, as an example.

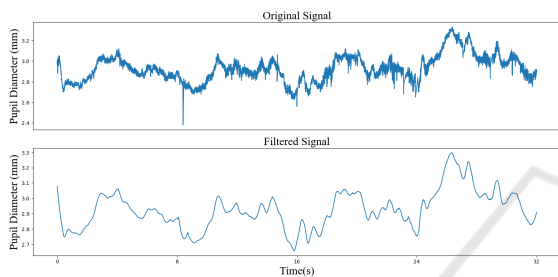


Figure 5: Comparison of original and filtered signals.

After the filtering stage, the signals go through a cut-off stage, removing the periods of the first and last cycles, resulting in signals of 16 seconds for the "Neutral" and "Blurry" effects and 18 seconds for the "Washout" effect. This cut-off is due to the pupil constriction effect at the beginning of each text reading, originated by the contrast change on the eye tracker screen, and by the noise present at the end of each signal, originated by participants who finished reading before the text presentation period was over. Figure 6 shows the result of this step.

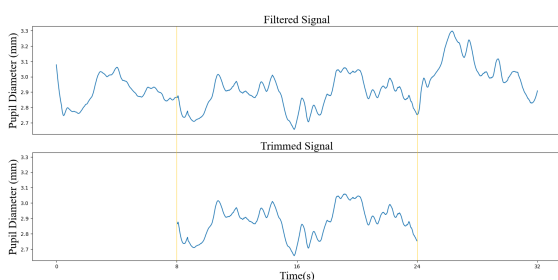


Figure 6: Comparison of filtered and trimmed signals.

The proposed pupil variation analysis was performed by averaging all signals of each stage of the experiment (Neutral, Blurry and Washout) to identify patterns in pupil diameter during the oscillations of the effects. For this, another data processing step was performed to obtain the normalized signal that con-

siders the change in pupil size from the first measurement of the first sample, so that the natural pupil size variables of each participant were excluded, subtracting the value of the first acquisition from the rest of each signal, obtaining a signal that always starts at zero, as shown in Figure 7.

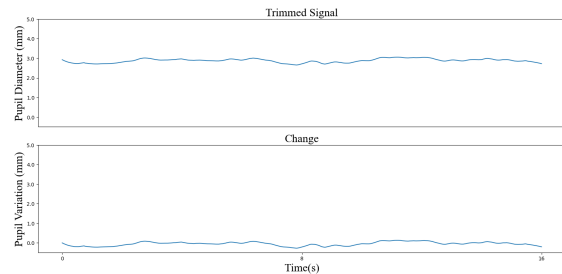


Figure 7: Change comparison.

3.5 Image Preprocessing

In addition to obtaining the change, the variance of the Laplacian of each frame of the videos generated with the visual distortions was calculated, so that they could be compared with the averages of the signals of each effect. Considering the frame image as I , of dimensions m and n , the method consists in applying the second derivative to detect negative edges in the image passing at high frequencies. The Laplacian operator can be approximated using the following mask (Pech-Pacheco et al., 2000):

$$L = \frac{1}{6} \begin{bmatrix} 0 & -1 & 0 \\ -1 & 4 & -1 \\ 0 & -1 & 0 \end{bmatrix} \quad (1)$$

Then the sum of all absolute values is calculated, to group the data at each point:

$$LAP(I) = \sum_m \sum_n |L(m,n)| \quad (2)$$

where $L(m,n)$ is the convolution of the frame image, using the mask L .

Then the variance of the absolute values is calculated, as shown below:

$$LAPVAR(I) = \sum_m \sum_n [|L(m,n)| - \bar{L}]^2 \quad (3)$$

where the mean is given by:

$$\bar{L} = \frac{1}{NM} \sum_m \sum_n |L(m,n)| \quad (4)$$

The values were related to the distortion variable presented earlier to control the intensity of the effects,

being adapted to "1" (maximum value, text with the most visual distortion) and "0" (minimum value, text without any visual distortion). The values obtained in each frame were also organized graphically, so that the cycles of distortions could be observed. In addition, the frames acquisitions during the experiment were transformed to the time scale.

Finally, the obtained signal also goes through a cutoff step, removing the periods of the first and last cycles, resulting in 16 second signals for the "Neutral" and "Blurry" effects and 18 seconds for the "Washout" effect, just as in the pupil signal preprocessing step.

3.6 Frequency Domain Analysis

From the data obtained in subsection 3.4 (Signal Pre-processing), the pupillary signals are separated by visual effect category, originating 3 groups, each with 50 signals, representing the signals acquired in the texts with "Neutral", "Blurry" and "Washout" effects, respectively. From these groups, the signals are organized into three matrices, where each row represents an individual signal and each column an eye tracker acquisition. From these matrices, each column is averaged, storing each average value in an index of a vector of the same dimension as the preprocessed signals. The result is three vectors that contain the average of the signals in each group, enabling graphical analysis.

From the average signals of each group and the signals of the visual effects cycles obtained in subsection 3.5 (Image Preprocessing), the frequency domain analysis of the signals is performed, by applying the Fast Fourier Transform (FFT), a fast algorithm for optimization of the Discrete Fourier Transform (DFT), a tool that performs the frequency analysis for discrete signals, to obtain the frequency spectra. The definition of the DFT is presented in the following equation:

$$X(m) = \sum_{n=0}^{N-1} x(n)e^{i2\pi nm/N} \quad (5)$$

where $x(n)$ constitutes the set of points representing the signal in time and N is the number of sampled points. Moreover, m is given by:

$$m = 0, 1, 2, 3, \dots, N - 1 \quad (6)$$

3.7 Pattern Recognition

In the pattern recognition step, a multivariate statistical technique consisting of reducing the dimensionality of the data (PCA) (Abdi and Williams, 2010) and applying Maximum Uncertainty Linear Discriminant

Analysis (MLDA) (Thomaz et al., 2007) is implemented to extract the discriminant information from the pupillary signals.

Initially, the data are organized in a matrix of dimension $N \times n$, in which N represents the total number of pupillary signals, having dimension 150 and n represents the size of pupillary signals, having dimension 4800 (the signal of the "Washout" group is compressed). It is then averaged and subtracted from all values, resulting in a matrix with zero average signal. Next, the PCA technique is applied to reduce the dimensionality of the data, obtaining the principal components matrix $n \times m$. This matrix is used as input to calculate the discriminant eigenvectors of MLDA, obtaining a $N \times k$ matrix with the most discriminant characteristics of each of the N input signals. This technique is presented in the diagram of Figure 8.

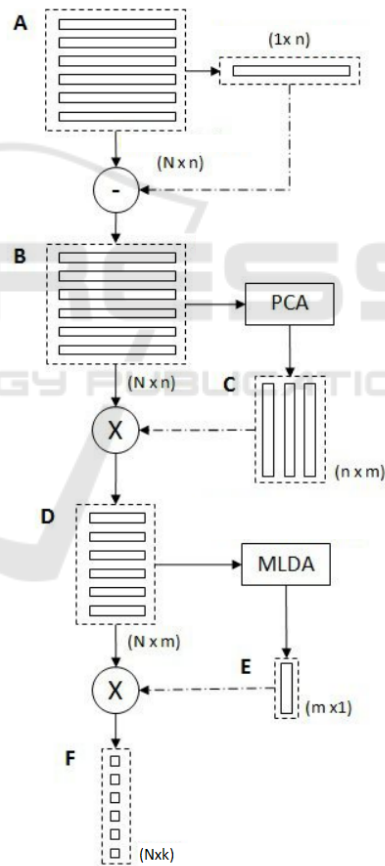


Figure 8: PCA + MLDA diagram.

4 RESULTS

The results of the comparison between the averages of the visual signals and cycles for each step of the

experiment are presented in Figures 9, 10 and 11 below.

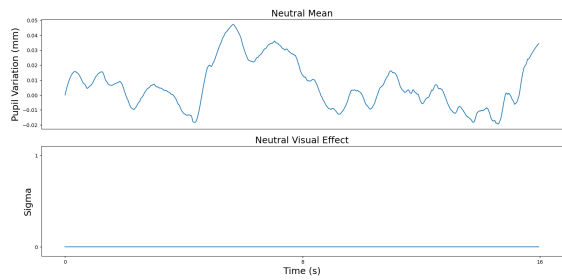


Figure 9: Comparison of Neutral mean signal and Neutral visual effect.

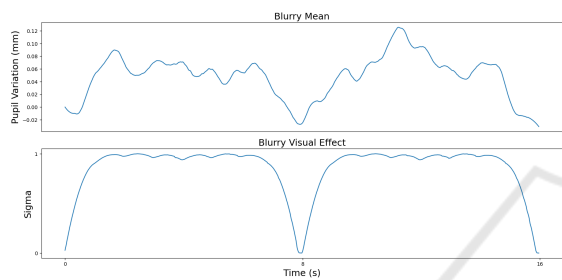


Figure 10: Comparison of Blurry mean signal and Blurry visual effect.

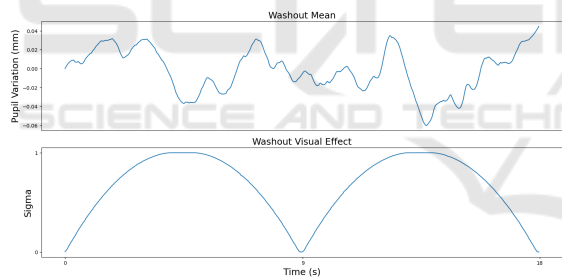


Figure 11: Comparison of Washout mean signal and Washout visual effect.

The results of the frequency analyses of the averages of the "Blurry" and "Washout" signals and the visual cycle signals of the respective effects are presented in Figures 12 and 13. The frequency domain analysis of the "Neutral" effect has no comparison because no distortions were present in the presented text.

The values noted in the spectrum represent the frequency of the harmonic components (X) and amplitude of the same components (Y).

Table 1 show the correlation between the average signals.

The results of the statistical pattern recognition step, using PCA and MLDA are presented below in 2D and 1D geometric forms (scatter) in Figures 14

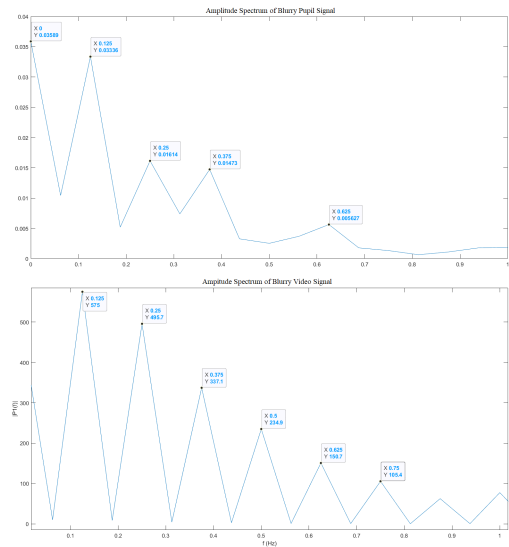


Figure 12: Frequency domain analysis for Blurry pupil signal and Blurry visual effect.

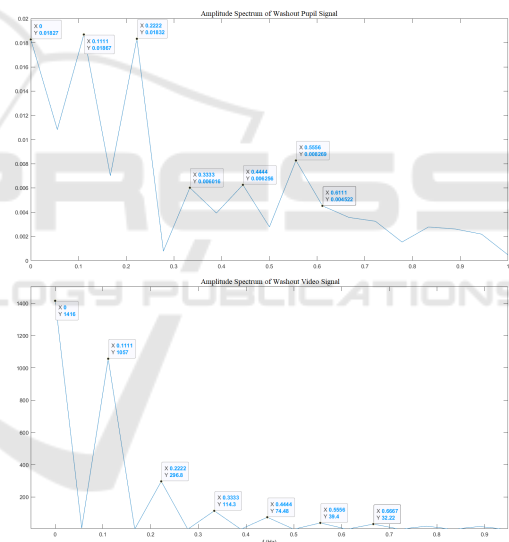


Figure 13: Frequency domain analysis for Washout pupil signal and Washout visual effect.

and 15. Figure 16 shows the confusion matrix between the classes, in which they are represented by: Neutral (1), Blurry (2) and Washout (3).

The overall accuracy of the classification using the methods described in subsection 3.7 showed an average accuracy of 66.67%.

5 DISCUSSION

As presented in Figures 9, 10 and 11, it is possible to note that for the Neutral effect, there were no cyclical

Table 1: Correlation between the average signals.

	Neutral	Blurry	Washout
Neutral	1	3.8e-2018	0
Blurry	3.8e-2018	1	0
Washout	0	0	1

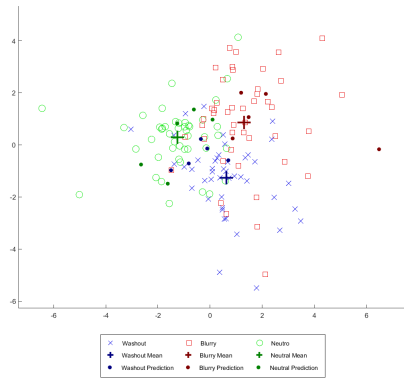


Figure 14: Dispersion relations for the three classes.

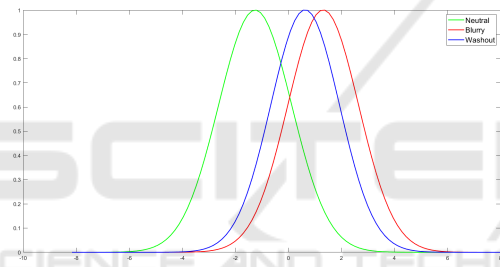


Figure 15: Dispersion curves.

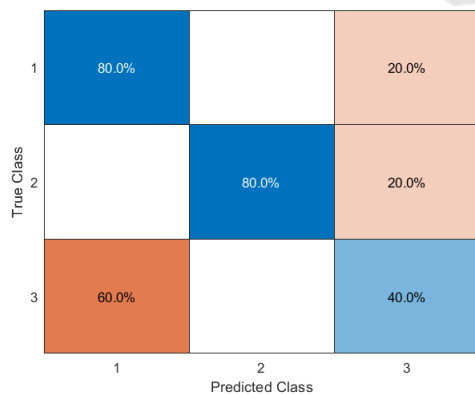


Figure 16: Confusion Matrix.

variations during the reading of the text. However, for the Blurry and Washout effects, it is possible to notice a cyclical behavior of the pupil diameter, varying in relation to the intensity of each effect.

This relationship can also be observed in the spectra of the signals, shown in Figures 12 and 13. The

pupil signals present fundamental harmonics with the same value, defining exactly the oscillation cycle of the visual effects. Furthermore, it is possible that the harmonics needed to reconstruct the signal coincide, varying only in amplitude.

For the Blurry effect, the increase in pupil diameter is due to increased difficulty in reading the text, which, when it reaches its maximum value, still allows reading, but with much greater difficulty, indicating increased attention and consequently increased mental effort required to complete the task (Hess and Polt, 1960) (Kahneman and Beatty, 1966) (Schluroff, 1982). For the Washout effect, the reduction in pupil diameter is due to the impossibility of reading at the moment when the text reaches its maximum value, indicating a state of rest and, consequently, a reduction in the mental effort required during these periods (Kahneman et al., 1967).

In the pattern recognition results, presented in Figures 14 and 15, the method did not show high classification accuracy, however, from Figure 15 it is possible to observe that the dispersion curve of the signals of the "Neutral" class stands out from the dispersion curves of the other classes, concluding that the pupillary signal during the reading of a text with visual effects has discriminating characteristics of the pupillary signals during the reading of texts without any effects.

In future work, it is intended to compare with other methods given that the present work was a first analysis of pattern identification in the context of pupil variation in MIS.

ACKNOWLEDGEMENTS

The authors would like to acknowledge the support of CAPES (funding code 001). Additionally, the authors would like to thank all the volunteers participating in the experiment.

REFERENCES

Abdi, H. and Williams, L. J. (2010). Principal component analysis. *Wiley interdisciplinary reviews: computational statistics*, 2(4):433–459.

Beatty, J., Lucero-Wagoner, B., et al. (2000). The pupillary system. *Handbook of psychophysiology*, 2(142-162).

Bergstrom, J. R. and Schall, A. (2014). *Eye tracking in user experience design*. Elsevier.

Bicalho, L. F., de ALMEIDA, M. Z. T., Guimaraes, M. R., Silva, J. R. G., and Fully, F. (2015). Síndrome de irlen: Um olhar atendo sobre o funcionamento cerebral du-

- rante a leitura. *Acta Biomedica Brasiliensia*, 6(1):35–44.
- Bremner, F. D. (2012). Pupillometric evaluation of the dynamics of the pupillary response to a brief light stimulus in healthy subjects. *Investigative ophthalmology & visual science*, 53(11):7343–7347.
- de Faria, L. N. (2011). Frequência da síndrome de meares-irlen entre alunos com dificuldades de leitura observadas no contexto escolar.
- Federal, G. (1990). Estatuto da criança e do adolescente. *Lei federal*, 8.
- Guimarães, M. R., Vilhena, D. d. A., Loew, S. J., and Guimarães, R. Q. (2020). Spectral overlays for reading difficulties: oculomotor function and reading efficiency among children and adolescents with visual stress. *Perceptual and Motor Skills*, 127(2):490–509.
- Hess, E. H. and Polt, J. M. (1960). Pupil size as related to interest value of visual stimuli. *Science*, 132(3423):349–350.
- Irlen, H. (2005). *Reading by the colors: Overcoming dyslexia and other reading disabilities through the Irlen method*. Penguin.
- Irlen, H. L. (1990). Method and apparatus of treatment of symptoms of the irlen syndrom. US Patent 4,961,640.
- Kahneman, D. and Beatty, J. (1966). Pupil diameter and load on memory. *Science*, 154(3756):1583–1585.
- Kahneman, D., Beatty, J., and Pollack, I. (1967). Perceptual deficit during a mental task. *Science*, 157(3785):218–219.
- Marieb, E. N. and Hoehn, K. (2007). *Human anatomy & physiology*. Pearson education.
- Marieb, E. N. and Keller, S. (2011). *Essentials of Human Anatomy and Physiology: Books a la Carte Edition*. Benjamin-Cummings.
- Orsi, R. N., Fabbro, D. A. D., and Thomaz, C. E. (2019). Eye-tracking data analysis during cognitive task. In *Latin American Workshop on Computational Neuroscience*, pages 200–219. Springer.
- Pech-Pacheco, J. L., Cristóbal, G., Chamorro-Martinez, J., and Fernández-Valdivia, J. (2000). Diatom autofocusing in brightfield microscopy: a comparative study. In *Proceedings 15th International Conference on Pattern Recognition. ICPR-2000*, volume 3, pages 314–317. IEEE.
- Romera, J. V. M., Orsi, R. N., Maia, R. F., and Thomaz, C. E. (2019). Visual patterns in reading tasks: an eye-tracking analysis of meares-irlen syndrome simulation effects. In *Anais do XV Workshop de Visão Computacional*, pages 131–136. SBC.
- Savitzky, A. and Golay, M. J. (1964). Smoothing and differentiation of data by simplified least squares procedures. *Analytical chemistry*, 36(8):1627–1639.
- Schluroff, M. (1982). Pupil responses to grammatical complexity of sentences. *Brain and language*, 17(1):133–145.
- Senior, K. R. et al. (2010). *The eye: the physiology of human perception*. The Rosen Publishing Group, Inc.
- Soares, F. A. and Gontijo, L. S. (2016). Production of knowledge: genetic basis, biochemical and immunological of meares-irlen syndrome. *Revista Brasileira de Oftalmologia*, 75:412–415.
- Thomaz, C. E., Boardman, J. P., Counsell, S., Hill, D. L., Hajnal, J. V., Edwards, A. D., Rutherford, M. A., Gillies, D. F., and Rueckert, D. (2007). A multivariate statistical analysis of the developing human brain in preterm infants. *Image and Vision Computing*, 25(6):981–994.